AUTOMATED PROCESSING OF ARCTIC CROWD-SOURCED HYDROGRAPHIC DATA WHILE IMPROVING BATHYMETRIC ACCURACY AND UNCERTAINTY ASSESSMENT

Khaleel Arfeen, Ian Church

Ocean Mapping Group

Department of Geodesy and Geomatics Engineering

University of New Brunswick, 15 Dineen Drive

P.O. Box 4400, Fredericton, N.B., E3B 5A3, CANADA

K.A@UNB.CA

Hydro 2019

Biloxi, Mississippi

Abstract

Melting sea ice has led to an increase in navigation in Canadian Arctic waters. However, these waters are sparsely surveyed and pose a risk to mariners. Recognizing this issue, the government of Canada has granted funds to develop a pilot program to begin collecting bathymetric data through a trusted crowd-sourced approach. As part of this project, the University of New Brunswick's Ocean Mapping Group is tasked with the processing of the collected data. Through an automated approach the software will process the data with the end product being a final depth measurement. The software has been broken down into several modules to complete the task at hand. This paper will delve into the global navigational satellite system (GNSS) and sound velocity profile (SVP) processing modules, including the methodologies and results.

Introduction

While it is unfortunate that climate change is causing the melting of Arctic sea ice, this is the current situation and some will find opportunities towards navigation in these waters. However, vast areas of the Arctic remaining unchartered to this day and this presents a liability towards navigational safety. The government of Canada is employing an untraditional approach to combat this predicament as traditional survey methods would be far too costly and timely to undertake. This initiative is a Crowd-Sourced approach where participating local communities are empowered with the choice of collecting crowd-sourced bathymetric (CSB) data while traversing their local waterways. Participants are given specialized hardware which can be towed from a watercraft while simultaneously collecting GNSS, motion and sonar data.

Apart from acquisition, to make this project feasible a system must be in place to efficiently process the data through automation while improving accuracy and assessment of uncertainty. To do so required a comprehensive workflow which spans from acquisition to dissemination. To make the processing more robust, the specific steps of the process have been modularized to do one thing and to do it well. These modules are visualized in the technical flowchart in figure 1.

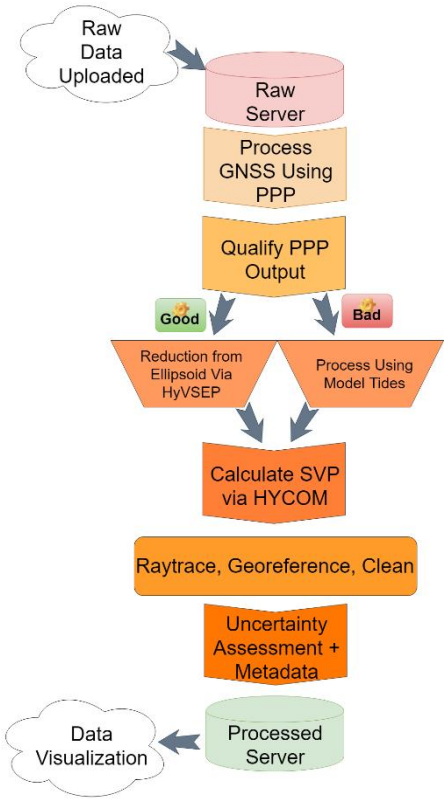

Figure 1 Technical Flowchart of the CSB Data Processing

The location information provided by the GNSS receiver plays a crucial role in positioning the sounder information. This includes latitude, longitude and height. Unfortunately, obtaining a strong GNSS signal is more stressed than at mid-latitude regions, but several methods exist to improve upon the accuracy of the GNSS reading. After the improvement has been made, qualification of the readings on a per-line basis is done to sort the lines on quality. If the quality meets threshold requirements, it is able to be used for vertical referencing.

When conducting a hydrographic survey, depth is never directly measured it is only inferred. We directly measure the time it takes for the sonar signal to propagate to the seafloor and back, known as the Two-Way Travel Time (TWTT). Combining the ½(TWTT) with incidence angle and sound speed, we are able to calculate depth (Mirjam Snellen, 2008). The speed of sound calculation is derived from temperature,

salinity and pressure/depth variables and is given as a function of depth (Beaudoin, 2009). This array of sound velocity vs depth data is known as the Sound Velocity Profile (SVP).

The SVP plays a crucial role in obtaining an accurate bottom depth calculation and it is important to have the input variables represented accurately. The objective of the SVP module is to utilize an appropriate oceanographic model which can provide the inputs to the speed of sound calculation for the Arctic survey region. Once the model has been selected, the scripts must then query the hydrodynamic model for the oceanographic data per input line while considering date, time and location. After the inputs to the speed of sound calculation have been retrieved, the conversion to sound velocity is made using a sound-velocity algorithm followed by creation of the final formatted SVP.

This paper will dive deeper into the development of qualifying GNSS readings on quality of data and the process of selecting the appropriate oceanographic model and sound-velocity algorithm along with the processing steps to obtain the final SVP.

Related Work

GNSS

Regardless of the method used to acquire hydrographic data, challenges occur when surveying in the Arctic. The primary challenges common across literature are obtaining valuable GNSS data and issues with obtaining accurate tidal heights and sound velocity profiles. Two great starting points towards understanding GNSS positioning and issues in the Arctic are Guide to GPS Positioning (Wells et al, 1999) and GNSS Use in the High Arctic: Issues and Solutions from a Canadian Perspective (Langley, 2009). The major issues of using GNSS in the Arctic compromises primarily of ionospheric and geometry errors. Jensen et al (2010) discussed these issues with intention to raise awareness and foster thoughts around the issues. The authors concluded that geometry issues can only be corrected by improving navigation system coverage in this region. Further conclusions stated that using multiple frequencies basically eliminated ionospheric delays, but high order effects still present an issue. Jayachandran et al (2009) reiterated the issues with ionospheric delays associated with GNSS in the Arctic and taking it further they described the concept of scintillation which has large temporal and spatial variance across the Arctic. The scientific research objectives of this paper were to assess the drivers and variabilities of polar cap convection and the generation and dynamics of ionization structures for which they concluded that more research needed to be completed. Finally, Reid (2015) explains GNSS integrity in the Arctic with particular emphasis on using Advanced Receiver Autonomous Integrity Monitoring (ARAIM) and Satellite Based Augmentation Systems (SBAS) as a potential aid to navigation and mapping in the Arctic. Reid explains that this is just

currently not feasible because of limitations in the GNSS constellations covering the Arctic. However, planned expansion is expected in the next decade and opens the possibility to further research including uses in vertical referencing for bathymetric surveys.

Sound Velocity Profile

It is always best practice to collect temperature and salinity values through in-situ casts while conducting a survey, though this is not always possible for varying reasons. In the case of this project, having the participants collect this data would add undue complexity as the participants are not hydrographers, would add considerable expense to the equipment package, and planning the deployment of additional equipment could interfere with survey operations. As a result, during processing of the data from this project we will obtain no observed sound velocity information and thus must supplement with the use of hydrodynamic models. When presented with a similar problem, Beaudoin et al (2006) has shown that the use of the World Open Atlas (WOA) model could be used appropriately to supplement the absence of observed SVPs without seriously affecting sounding accuracy in the Arctic. Church et al (2012) has shown that model output could be used as a substitute for actual observations with little effect on ray-tracing uncertainty. Furthermore, the authors stated that a model can be used to learn about the temporal distribution of salinity and temperature in comparison to a single point as when taking a traditional cast. This aids in survey planning and the use of a model would improve survey efficiency and uncertainty. To further this thought, Calder et al (2004), has shown that using models could bring down operational costs of conducting surveys by avoiding taking casts. In their study, these authors have shown that a model-based SVP can be used within the budget error of International Hydrographic Organization (IHO) standards. However, the authors did specifically mention that more studies are necessary when working in shallow environments (0-30m) to determine if a model is suitable.

Once a model has been chosen with appropriate spatial and temporal coverage, the temperature, salinity and depth variables are able to be retrieved. At this point a conversion of these inputs to a final sound velocity in water is needed. There exist multiple equations to perform this conversion, some more specialized to certain applications than others. These are available in literature from authors such as (Chen & Millero, 1997), (Grosso, 1974), (Mackenzie, 1981), (Wilson, 1960) and (Medwin, 1975). Pike and Beiboer (1993) has made a comparative study of several different algorithms along with recommendations. For water with depths less than 1000m the Chen and Millero equation is recommended by these authors. While the Chen and Millero equation has been adopted for many years as standard, in 2009 the Intergovernmental Oceanographic Commission (IOC) adopted the TEOS-10 equation. This equation now stands as the official descriptor of seawater and ice properties in marine science. Significant changes

introduced in this formula are the use of Absolute Salinity along with introduction of units to Ocean salinities (g/kg) (Intergovernmental Oceanographic Commission, 2010). It is commonly accepted that the greater the accuracy in determining the sound-velocity, the greater that accuracy carries forward into the final depth measurement (Alkan, Kalkan, & Turkiye, 2006) and the appropriate selection of the correct equation is important.

In order to assess the validity of the SVP, Beaudoin et al (2006) has laid out some methods on the comparison between observed SVPs and model derived SVPs. In this case it is necessary to compare the model-derived data to a 'true' dataset. The two profiles can be directly compared by plotting both into one depth-velocity graph. However, it can be taken further by completing the raytracing using both profiles independently to calculate depth. When plotting these results, the real-world implication of the associated error can be made when comparing to a known bottom depth.

Methodology

Process GNSS data via Precise Point Positioning (PPP)

The HydroBall is able to capture both L1 and L2 GPS frequencies as well as GLONASS signals. However, there are significant challenges surrounding obtaining accurate readings in a predominately Arctic survey setting when compared to reading obtained at mid-latitudes. The main challenges in resolving an accurate GNSS reading occur primarily from poor satellite-receiver geometry and ionospheric effects (Jensen & Sicard, 2010).

Due to low inclination angles of GPS and GLONASS constellations, the Satellite geometry is never favorable in the Arctic and satellites will reside close to the horizon, see figure 2. The factor known as the Geometrical Dilution of Precision (GDOP) is a term used to capture the GNSS geometry in 3D position and time. A higher GDOP reading indicates a poorer satellite geometry and in turn negatively influences the ultimate positioning accuracy (Wells, et al., 1999), see figure 3. The DOP acts as a multiplier towards measurement accuracy, meaning we want to minimize these effects as much as possible to obtain the most accurate position (Wells, et al., 1999).

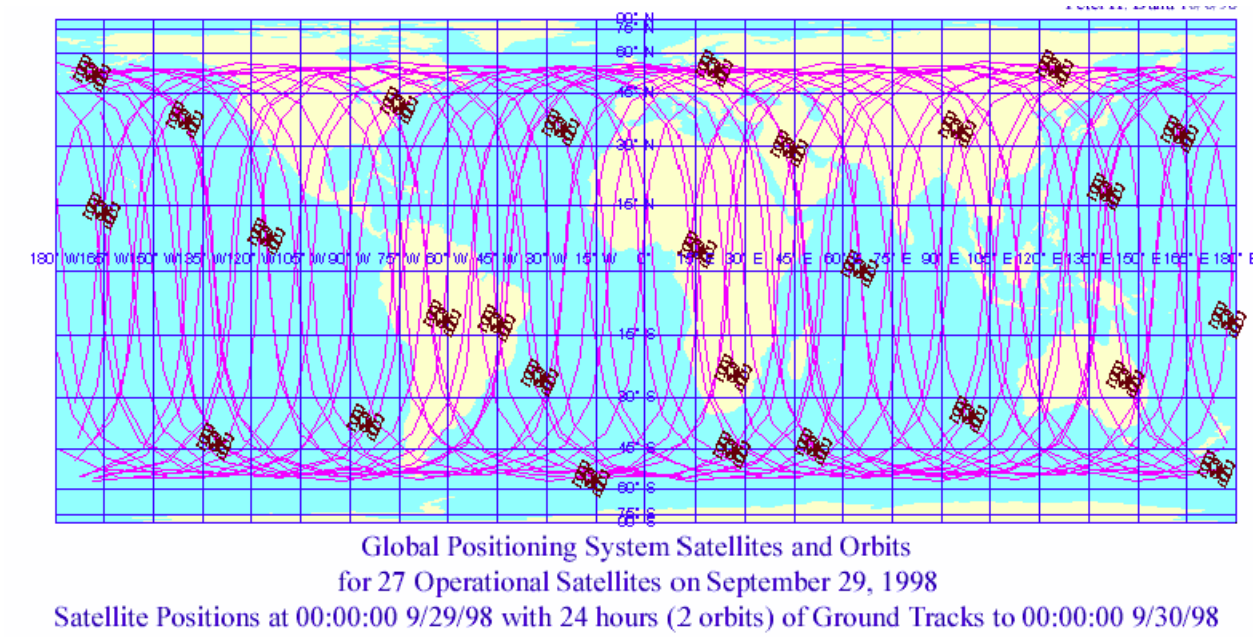

Figure 2 GPS satellite Ground Track (55 degree inclination) src: colorado.edu

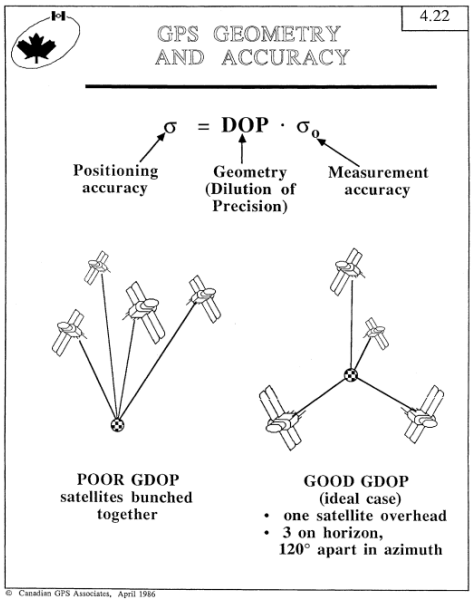

Figure 3 GNSS Geometry (DOP) src: Wells et al, 1999

Ionospheric errors also play a crucial role at higher latitudes when we have low satellite elevation (Monge, Clara de Lacy, & Radicella, 2011). While it is true that dual-frequency receivers correct first-order ionospheric effects almost completely, higher order effects are not handled (Jensen & Sicard, 2010). These higher order ionospheric errors are a function of the electron density distribution and the magnetic field vector along the GPS signal propagation path (Matteo, Morton, Chandrasekaran, & Van Graas, 2009). These higher order ionospheric effects can cause errors of more than 10cm.

To obtain a greater positional accuracy, post-processing of the GNSS data must be completed. Several methods exist to help obtain a greater positional accuracy such as Differential GNSS (DGNSS), Real Time Kinematic (RTK), Post Processed Kinematic (PPK) and Precise Point Positioning (PPP). Due to the increased complexity of setup (base station needed), distance restrictions and associated costs involved with DGNSS, RTK and PPK solutions, PPP was chosen as the post-processing method. It can be shown that PPP provides an excellent

performance especially when using final orbits to generate the final solution (Malinowski & Kwiecien, 2016), negating many of the benefits of using a differential system as well as providing simplicity for the operator. PPP is able to provide a sub decimeter accuracy with dual frequency kinematic readings (Huber, et al., 2010). However, PPP does have a longer convergence time that will need to be accounted for.

There are several choices of systems available to run the PPP processing including RTKLIB, UNB GAPS and NRCAN PPP. Each of these systems provides roughly the same output, however NRCAN PPP was ultimately chosen. This is because GAPS does not support GLONASS which is deemed necessary for the project as GPS inclination is limited for the project region. RTKLIB was not able to take GLONASS into account when converting the raw GNSS readings from the Hemisphere format to Rinex. The NRCAN PPP system allows for several different methods of submission. Keeping our automation goals in mind a python script utilizes a WGET method to submit RINEX files to their server and then fetches the results.

The final output of the NRCAN PPP service is provided as a .zip file containing of importance a .pdf summary of the processing, a .sum of the processing parameters summary, an errors.txt file outlining errors and warnings which occurred during processing and a .pos file which contains the actual position information.

While PPP no doubt improves our GNSS readings it does come with limitations. The primary limitation is the long convergence time needed to obtain a solution (Approximately 10-30 minutes). Surveying in the Arctic does present its own limitation, particularly on higher degree ionospheric errors, satellite geometry, topographic zenith delay and multipath errors, which add to uncertainty and loss of accuracy in the GNSS readings. Additionally, in cases where we cannot resolve even a poor GNSS reading, the PPP processing will reject these readings and are documented in the .sum file. As shown there are limitations when using GNSS for some of which we can help to mitigate, others we cannot. Either way, it is important to document these limitations in the metadata so that the final user obtains a transparent explanation of the limitations and challenges with this data.

Qualify the GNSS PPP output via a threshold filter

Once the location data has been processed using PPP, the GNSS reading is then placed under a threshold filter to sort acceptable vs. non-acceptable readings on a per line basis. This step is crucial since vertical height is of utmost importance and poor GNSS readings will hinder the accuracy of the final depth sounding. If the GNSS reading is acceptable we will use the ellipsoidal vertical height otherwise we will need to estimate vertical height through a hydrodynamic tidal model and a traditional water level reference approach. To filter the results a combination of six threshold variables were chosen. These variables are

number of satellite vehicles (NSV), geometric dilution of precision (GDOP), standard deviation of latitude (SDLAT), standard deviation of longitude (SDLON), standard deviation of height (SDHGT) and standard deviation of clock (SDCLK). The minimum standard deviation values chosen for latitude, longitude and height are 5.0m, 5.0m and 0.5m respectively. These values were chosen to maintain a CHS level 1a survey standard. The maximum GDOP value selected is 3.5 which according to Langley (1999) is considered an excellent rating, see figure 4. The GDOP threshold value may be changed later to reflect a good value (4-6) which would be sufficient for the project. The minimum NSV value selected is 6 and the standard deviation of the clock is 3. The NSV and SDCLK values will be selected with more precision after further testing. All values can be adjusted to be more or less lenient depending on requirements.

DOP Value	Ratings
1	ideal
2-4	excellent
4-6	good
6-8	Moderate
8-20	Fair
20-50	poor

Figure 4 DOP Ratings src: Langley, 1999

Using these threshold values, each reading is sorted on a line-by-line basis and then put into a .srt file which splits the GNSS readings as acceptable or not-acceptable. Some limitations of this step are that it is necessary for the system to be able to keep track of which readings obtained the vertical reference from GNSS or from tidal models and include this in the metadata. This tracking and documenting adds a layer of complexity to the system. Also, it is difficult to come up with a one-size fits all approach to threshold values, however using the outlined values this should provide a consistent criteria for filtering.

Sound Velocity Profile

Ideally, we would be able to directly calculate sound speed with in-situ casts done while surveying. Due to project constraints towards operator simplicity this is not an option and thus sound speed will be derived from oceanographic models. When selecting a model, we must be able to have accurate temperature and salinity readings throughout the water column and the model coverage must extend to the surveying locations of this project at an acceptable temporal and spatial resolution.

Three model candidates that have Arctic coverage were selected, being World Ocean Atlas 18 (WOA18), Real Time Operational Global Ocean Forecast System (RTOFS) and Hybrid Coordinate Ocean Model (HYCOM). While HYCOM and RTOFS are numerical baroclinic hydrodynamic ocean models, the WOA18 is a collection of in-situ oceanographic data. As a result the WOA18 data does not provide the

same temporal resolution of the HYCOM and RTOFS data except on an annual, seasonal and monthly scale, where values are interpolated across the grid (National Oceanic abd Atmospheric Administration, 2019). After careful contemplation, the HYCOM model was ultimately chosen for its sufficient Arctic coverage, archive access and Thredds server support as summarized in table 1. The HYCOM model can provide archived data, nowcasts (current state) and forecasts of oceanic parameters, this includes three-dimensional data for temperature, salinity and depth (Metzger, et al., 2014).

Table 1 Summary of Comparisons between the three candidate Ocean Models

	HYCOM (GOFS 3.1)	WOA18	RTOFS
Temperature, Salinity, Depth Available	Yes	Yes	Yes
Horizontal Resolution	0.08 deg lon x 0.08 deg lat (40S-40N); 0.08 deg lon x 0.04 deg lat (poleward)	0.25 deg lon x 0.25 deg lat (60N-90N)	0.08 deg lon x 0.08 deg lat
Vertical Resolution	0m-5000m	0m-4000m	0m-4000m
Temporal Resolution	3 hours	Annual, Seasonal, Monthly	3 hours
Access	Thredds, FTP, OpenDAP, NetCDF, HTTPS	Thredds, HTTPS, FTP, GeoPortal, NetCDF, Live Access Server	FTP, NetCDF, OpenDAP, HTTPS
Archive Access	Yes	Yes, limited	No
Arctic Support	Yes	Yes	Yes
Automation Support	Yes	Yes, limited	Yes

Once the model was selected, scripts were then written on interacting with the model through the Thematic Real-time Environmental Distributed Data Services (THREDDS) server. HYCOM has several different model domains to choose from each covering different areas with differing resolution. The chosen domain was the Global Ocean Forecasting System (GOFS 3.1) specified with GLBv0.08 resolution. The specifics towards this domain are provided in table 2. To collect the necessary temperature and salinity data arrays needed to calculate the sound velocity, the HYCOM model requires inputs of date, time, latitude and longitude for the area of interest. These inputs are obtained from the .srt file created in the GNSS module upstream. The .srt file contains potentially hundreds to thousands of lines with unique data values. To minimize queries being sent to the HYCOM server, it was necessary to create a query cache. This is necessary because the HYCOM model does not directly accept the real

values obtained from the .srt file, instead requiring conversion to their proprietary index to obtain results. A summary of the conversions necessary for date, time, latitude and longitude are provided in table 3. Due to the model resolution limits, identical queries may be produced for input data close in space and time proximity. This would be burdensome to processing efficiency and the THREDDS server to run each query individually and hence why the use of a cache is needed.

Table 2 Summary of GOFS 3.1 Specifications (src: https://www.hycom.org/dataserver/gofs-3pt1/analysis)

	HYCOM (GOFS 3.1)
Title	Global Ocean Forecasting System (GOFS 3.1)
Grid	GBLv0.08
Span	80S - 90N
Data Range	July-2014 - Present
Frequency	3 hours
Horizontal Resolution	0.08 deg lon x 0.08 deg lat (40S-40N); 0.08 deg lon x 0.04 deg lat (<40S & >49N)

Table 3 Required conversions of input parameters for HYCOM Salinity and Temperature Query

Latitude Hycom Map

Index Range:	[0:3250]	
index	value	step
0-1000	(-80) - (-40)	0.04°
1000-1500	(-40) - (0)	0.08°
1500	0	0.08°
1500-2000	(0) - (40)	0.08°
2000-3250	(40) - (90)	0.04°

Time Hycom Map

* Hours since epoch (2000-01-01 00:00:00)

Index Range:	[0:T]	T updates every hour
index	value	step
0	157812	3.06h

Longitude Hycom Map

* Degrees East

Index Range:	[0:4499]	
index	value	step
0	0	0.08°
4499	359.92	0.08°

Depth Hycom Map

Index Range:	[0:39]	
index	value	step
0	0	Xm
39	5000	non-linear

Unique queries are then ran against the HYCOM model providing data arrays for Salinity-Depth and Temperature-Depth. In the case where null data is returned by the model a radial search function is executed, finding the nearest-neighbour with non-null data. The search function works by using a counter

and index to iteratively search a radius from given location by one step. The function starts off going up from the center by the step size. If this fails it returns to the center and goes right by one step size. This is repeated going down and to the left respectively. If no data is returned, the function will then search the diagonals, beginning with going up and to the right of center by one step size, down and to the left of center by one step size, up and to the left of center by one step size and down and to the right of center by one step size. If these queries fail, the step size is increased by one and the search is repeated until data is found. Note that the radial search only applied to the location, date and time are held constant during the process.

After retrieval of the temperature and salinity arrays, the data must be converted from HYCOM values to real world values to calculate the sound velocity. The conversion factor is provided in figure 5. Once converted, the temperature and salinity arrays are combined with latitude and longitude values and the sound velocity is calculated using the TEOS-10 algorithm. The significant change that occurs with TEOS-10 when compared the traditional methods is that the use of Absolute Salinity is adopted over Practical Salinity when describing the content of salt in seawater. Absolute Salinity is the mass fraction of salt in seawater and has units of g/kg whereas Practical Salinity is the measure of conductivity of seawater and is unitless. This has numerous advantages which can be found in the TEOS-10 manual (Intergovernmental Oceanographic Commission, 2010), with the primary benefit being increased accuracy from the use of Practical Salinity. The main disadvantage to the TEOS-10 algorithm is the complexity of the algorithm, making it unfeasible to derive our own implementation. Fortunately, a python implementation is freely available in the Gibbs-SeaWater (GSW) Oceanographic Toolbox Libraries, which provided the functions to convert Practical Salinity to Absolute Salinity and to perform the TEOS-10 sound velocity calculation. The final sound velocities are formatted as velocity-depth arrays.

Finally, the output is formatted as a Caris SVP file and saved in the working directory. This file format is described in figure 6. Under the comment section, the lines which the SVP are applicable to in the .srt are given as well as the query used to generate the data from HYCOM. A SVP file is created for each unique sound velocity profile which is derived from each unique HYCOM query.

```
sal = (int(sal) * 0.001) +20 #convert from hycom value to real value
temp = (int(temp) * 0.001) +20 #convert from hycom value to real value
```

Figure 5 HYCOM value to real world value conversion chart

```
[SVP_VERSION_2]
testOutFile.svp
Section 2018-214 17:33:18 68:38:24 -94:09:36 Add a Comment
0.00    1439.30
2.00    1439.18
4.00    1439.06
```

Line 1: specified SVP file version
Line 2: name of file
Line 3: year-Julian date time latitude longitude comment
Line 4-6+: depth velocity

Figure 6 Caris SVP File Format Specifications

The challenges associated with collecting accurate SVP involve model limitations and sound velocity conversion. Resolutions for the model grid are not ideal in both location and time, leading to inaccuracies. More so, truthing the model data is very difficult as it requires in-situ casts which are difficult and costly to obtain. Limitations when converting to sound velocity are that we must be trusting of the algorithm chosen. The sound velocity algorithm and chosen model should be the best selection for the area of interest and ideally would be applicable universally across survey regions. To communicate transparency to the final user, metadata should include the uncertainty associated with the chosen SVP model obtained through comparison with observed data, limitations of the search and query functions and the sound speed calculation used.

Discussion of the Results

GNSS

While many studies exist on the benefits of additional processing on GNSS readings, something that had not been investigated thoroughly was the benefits or drawbacks on using a single constellation (GPS) versus using multiple constellations (GPS + GLONASS) in the Arctic. To make this assessment, 22 raw GNSS datasets were obtained for on-site recordings in the Arctic collected by the Hydroball. The locations ranged from Gjoa Haven, Baffin Island to Greenland, as shown in figure 7. The timespan for the data was December 2017 to October 2018 and included kinematic and stationary data. The data was then processed using the regular workflow of PPP and the sorted using the qualification scripts.

Figure 7 Location of GNSS Dataset

Once processed, the each of the 22 datasets were summarized into a mean and standard deviation for the file. The mean and standard deviations of each of these 22 datasets were then used to create a single mean and standard deviation for each of the qualification metrics. The findings are shown below in table 4. We can see from the table that on average the NSV and GDOP values are more favourable when using both constellations, as expected. For the most part the rest of the variable are consistent amongst both options, with the exception of the clock standard deviation, showing some variance.

Table 4 Summarized Qualification Metrics

	Number Satellites Visible (NSV)		Geometric Dilution of Precision		Standard Deviation LAT(95%) (m)	
	GPS+GLONASS	GPS Only	GPS+GLONASS	GPS Only	GPS+GLONASS	GPS Only
Mean	12.54	8.84	1.90	2.45	0.17	0.19
Stdev	1.28	0.89	0.25	0.45	0.13	0.14
Max	15.39	10.74	2.50	4.04	0.50	0.52
Min	10.42	7.32	1.55	1.82	0.05	0.04
	Standard Deviation LON(95%) (m)		Standard Deviation HGT(95%) (m)		Standard Deviation CLK(95%) (ns)	
	GPS+GLONASS	GPS Only	GPS+GLONASS	GPS Only	GPS+GLONASS	GPS Only
Mean	0.17	0.17	0.32	0.34	1.22	0.94
Stdev	0.11	0.11	0.24	0.27	1.28	0.67
Max	0.36	0.40	0.87	1.00	5.15	2.38
Min	0.04	0.03	0.08	0.08	0.24	0.22

A chart was created to summarize the qualification parameters towards location in figure 8. We can see again that the data is relatively the same amongst the two. We do see a higher maximum for the standard deviation of height with the GPS only measurement.

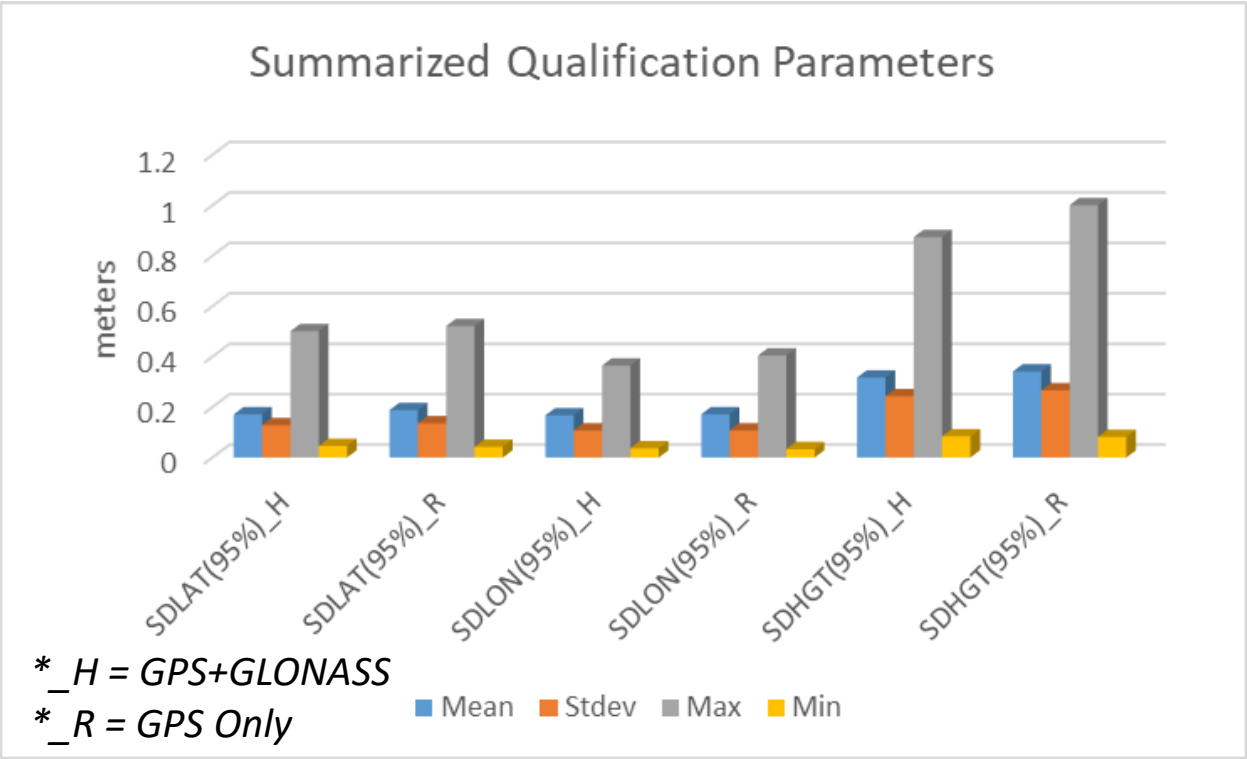

Figure 8 Summarized Qualification Parameters

Both datasets were then taken and processed using PPP and then qualified. Each dataset was then analyzed and a final pass rate for all the lines in the set was created. This is shown in figure 9, where a number of interesting finding can be inferred. Overall all location values are favorable with the use of GLONASS in addition to GPS. This did come at the expense of an increase in the clock standard deviations. A slightly higher pass rate was seen when using both constellations but not by a significant amount. On days where the GPS signal was poor (ie. 15_41_04-2018_10_21-gps &15_45_32-2018_10_21-gps), there was a qualification rate of 0% in the GPS only data. However, when adding GLONASS support we were able to actually use this data and bring up the overall qualification rate to 88% and 96% respectively. For this factor alone, it may be a better choice to use both constellations. The final average pass rate for all data was 84.6% for GPS and GLONASS observations and 74.7% for GPS Only.

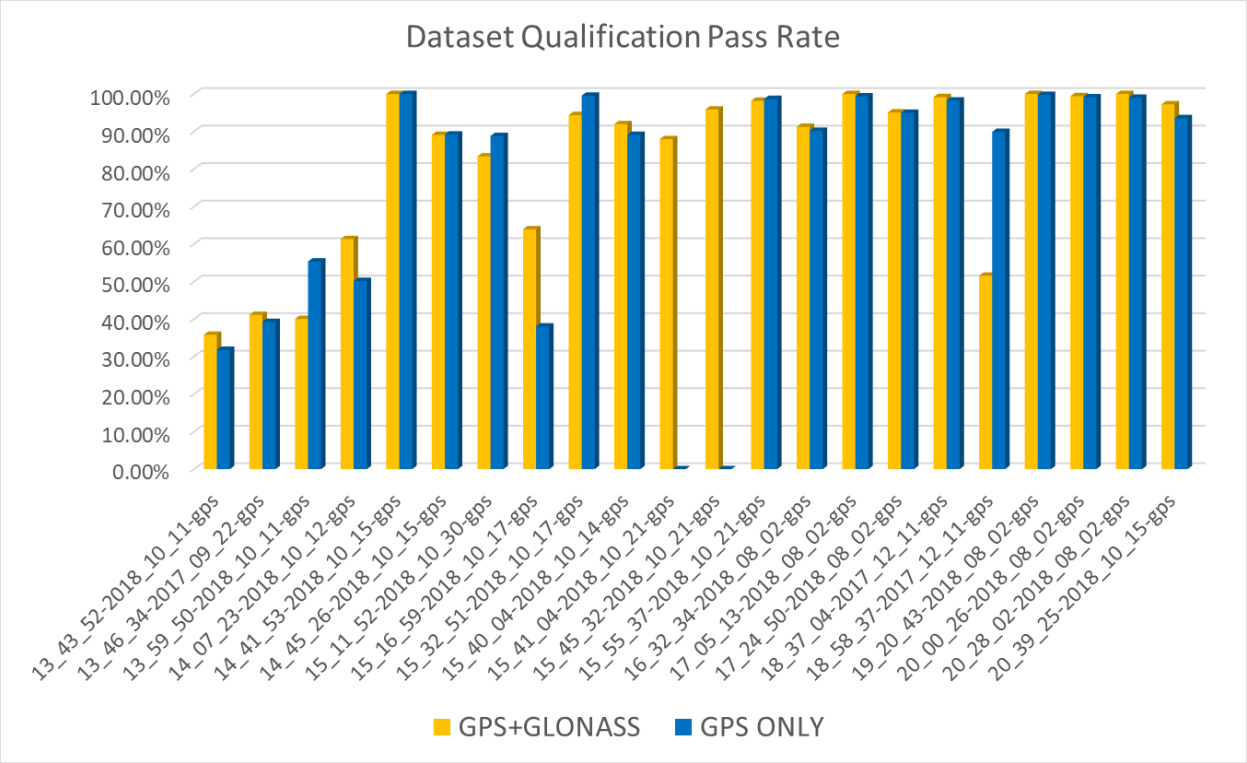

Figure 9 Dataset Qualification Pass Rate

Sound Velocity Profile

To help assess the accuracy of the HYCOM model data, real CTD casts were gathered from the Canadian Coast Guard vessel, the Amundsen. The data used was collected in various locations across the Canadian Arctic in the year 2017. The observed CTD casts were filtered to include only data with depths of 100m or less as this is the vertical capability limit of the hardware employed in this project. In total there are 17 CTD casts which serve as the 'truth'. The locations of these casts are visualized in figure 10 and metadata is shown in table 5. Comparable HYCOM data was collected based on the time, date and location of the CTD cast. All data will be formatted into three fields, depth (m), temperature (°C) and salinity (ppt). A comparison of the Salinity, Temperature and Depth data was made through correlation, graph visualization and differential comparison. Following this, the data was converted to SVPs and a further comparison was made on the depth error when used to raytrace.

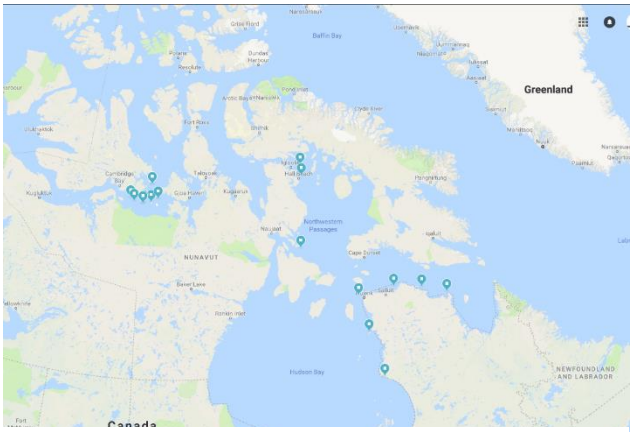

Figure 10 Location of Observed CTD Casts (courtesy of Google)

Table 5 Metadata for Observed CTD Casts

Cruise+Cast	date	depth	lat	lon
1702b-95	8/13/2017 19:14	16	68.7668	-80.841
1702b-89	8/9/2017 17:03	28	68.4906	-99.8955
1702b-87	8/9/2017 5:23	41	68.3279	-102.94
1702b-94	8/13/2017 16:17	42	69.2716	-80.6078
1702b-92	8/10/2017 9:22	52	69.1691	-100.695
1702b-91	8/10/2017 5:45	53	69.1707	-100.705
1702b-86	8/9/2017 0:31	55	68.4862	-103.429
1702a-3	7/9/2017 16:45	75	60.6961	-78.5643
1702a-2	7/8/2017 22:03	76	58.4258	-78.3035
1702b-90	8/9/2017 22:14	81	68.3061	-100.802
1702a-4	7/10/2017 9:10	86	62.5129	-78.4889
1702b-96	8/15/2017 7:17	89	65.451	-83.2584
1702a-7	7/11/2017 19:31	90	61.0419	-69.7163
1702b-85	8/8/2017 12:48	91	68.2471	-101.811
1702a-5	7/10/2017 21:00	92	62.3669	-74.662
1702a-6	7/11/2017 9:09	92	61.7868	-71.9121
1702b-88	8/9/2017 12:09	94	68.2426	-101.795
1702b-84	8/8/2017 9:08	97	68.3027	-101.738
1702b-83	8/8/2017 6:06	99	68.3028	-101.745

After the 17 casts of observed data had been collected and formatted, HYCOM model queries were created to obtain model casts for the same locations and time. To be able to compare the two datasets, some modifications needed to be made. The observed casts have a vertical resolution of 1m while the model cast's vertical resolution is more course at a range of 2m up to 10m intervals. To make a fair comparison, the model data was converted to the 1m scale keeping the value constant for the range. Additionally, NaN values in the observed dataset were ignored if occurring as the first or last value in the casts. In the 1702_086 dataset a series of NaN values were observed in the salinity readings between 5-7 meters. In this case the NaN values were replaced with a linear average between the 4 and 8 meter values. Finally, when the length of the dataset did not agree between the observed and model, the last model value was held constant and extended to the length of the observed cast. In the case where the model cast length was extended beyond the model, the extra data was ignored.

Now the two datasets could be compared and to do so a Pearson Product-Moment Correlation (r) value was calculated to compare the salinity and temperature values across each dataset, as shown in table 6 and figure 11. From the table we can see that the maximum correlation for temperature and salinity is 0.94 and 0.96, the minimum correlation is -0.90 and -0.96 and the average correlation is 0.44 and 0.57 respectively. We can see that salinity tends to be better correlated between the observed and model data than temperature. There were three temperature datasets with negative correlations, two salinity datasets with negative correlation and one salinity dataset with no correlation.

It is expected that the correlation between the two datasets will have a weak to strong positive correlation and the average values meet these predictions. What was not predicted was the negative correlation between datasets, especially present in the 1702-002 and 1702-089 datasets. When examining these values, it appears that the model values for these two datasets extend straight down, when compared to a wider ranged value for the observed data. A comparison of the highest and lowest correlated datasets are shown in figure 12 and 13. In either case the correlation values did not show any noticeable pattern in location or depth, as both shallow and deep casts had a mix of high and low correlation values.

Table 6 Observed vs. Model Temperature and Salinity Correlation Values for Each Dataset

Dataset	Correlation Temperature	Correlation Salinity
1702-002	-0.551	-0.815
1702-005	0.870	0.928
1702-006	0.709	0.783
1702-007	0.867	0.881
1702-083	0.605	0.770
1702-084	0.553	0.758
1702-085	0.546	0.805
1702-086	0.583	0.905
1702-087	0.805	0.964
1702-088	0.561	0.800
1702-089	-0.895	-0.957
1702-090	0.723	0.672
1702-091	0.900	0.944
1702-092	0.856	0.934
1702-094	-0.403	0.447
1702-095	-0.231	-0.010
1702-096	0.942	0.943
Max	0.942	0.964
Min	-0.895	-0.957
Mean	0.438	0.574

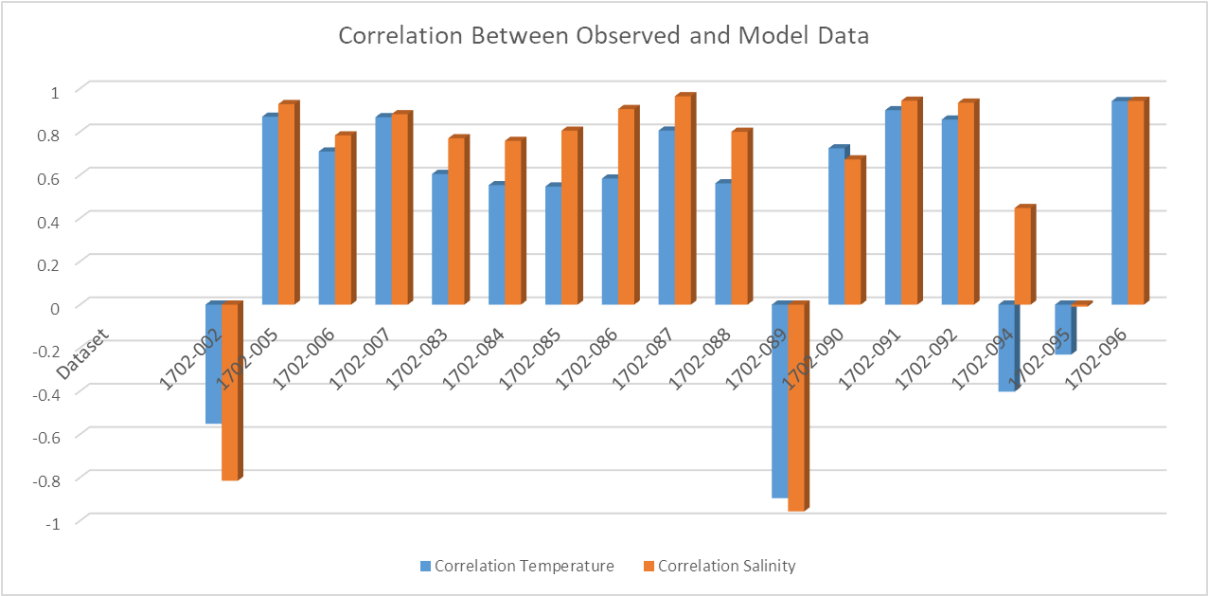

Figure 11 Correlation between Observed and Model Temperature and Salinity Values

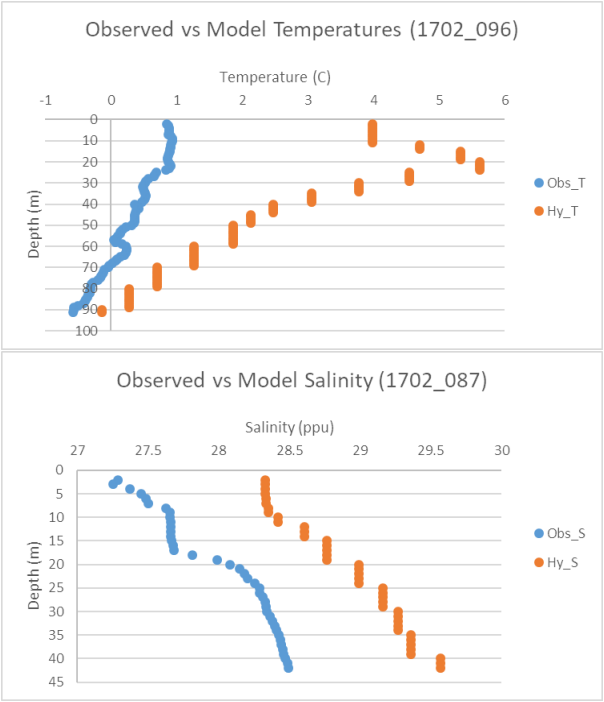

Figure 12 Highest Correlated Temperature and Salinity Graphs

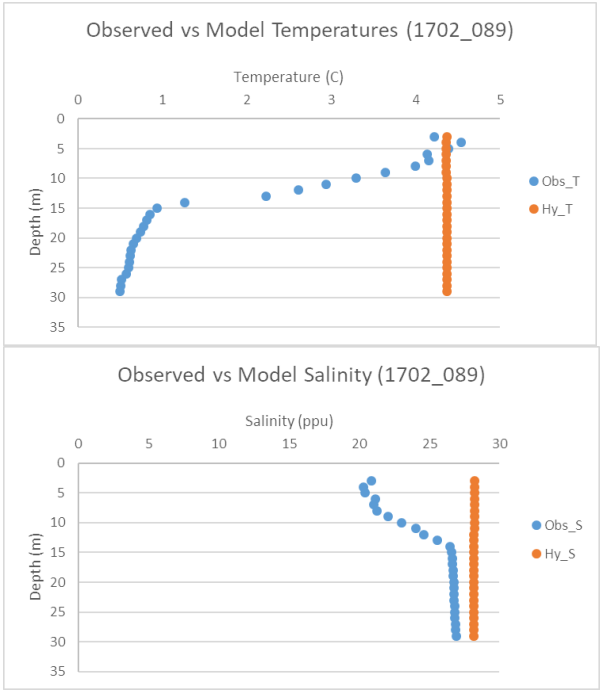

Figure 13 Lowest Correlated Temperature and Salinity Graphs

To further the analysis, the differences between the observed values and model values were calculated. Table 7 shows the results per dataset. Here we can see that the mean temperature difference across all 17 datasets is -2.24ºC with a standard deviation of 1.74 ºC and the mean salinity difference across all datasets is -0.91 ppt with a standard deviation of 1.06 ppt.

Table 7 Temperature and Salinity Differences between Observed and Model Salinity and Temperature Values

Dataset	**Δ Temperature (oC)**		**Δ Salinity (ppu)**	
	Mean	Stdev	Mean	Stdev
1702-002	-3.374	2.340	-0.996	0.855
1702-005	-1.613	0.574	-1.147	0.137
1702-006	-1.186	1.004	-0.344	0.645
1702-007	-1.529	1.390	0.147	0.445
1702-083	-1.992	1.845	-1.461	0.814
1702-084	-2.126	1.899	-1.447	0.793
1702-085	-2.224	1.669	-1.311	0.607
1702-086	-4.755	1.269	-1.302	0.106
1702-087	-3.350	2.210	-0.903	0.110
1702-088	-2.748	1.754	-1.198	0.476
1702-089	-2.463	1.559	-3.301	2.537
1702-090	-2.915	1.798	-1.680	2.097
1702-091	-1.682	0.404	-1.003	0.184
1702-092	-1.651	0.605	-0.980	0.222
1702-094	-0.809	0.195	0.839	0.058
1702-095	-0.672	0.163	-0.034	0.077
1702-096	-2.231	1.326	0.499	0.548
Mean(P)	**-2.244**		**-0.915**	
Stdev(P)	**1.737**		**1.057**	

To get a depth dependent difference in temperature and salinity, values for all casts were grouped together in 10m intervals. Since not all casts were equal in depth, a frequency distribution graph was created to show the number of values per depth range in figure 14. The mean and standard deviations of the differences between observed and model temperature and salinity values were then calculated and show in figure 15 and 16. We can see that the highest mean difference between the two datasets occurs in the 20-39 m depth range for temperature and between the 0-9 m depth range for salinity.

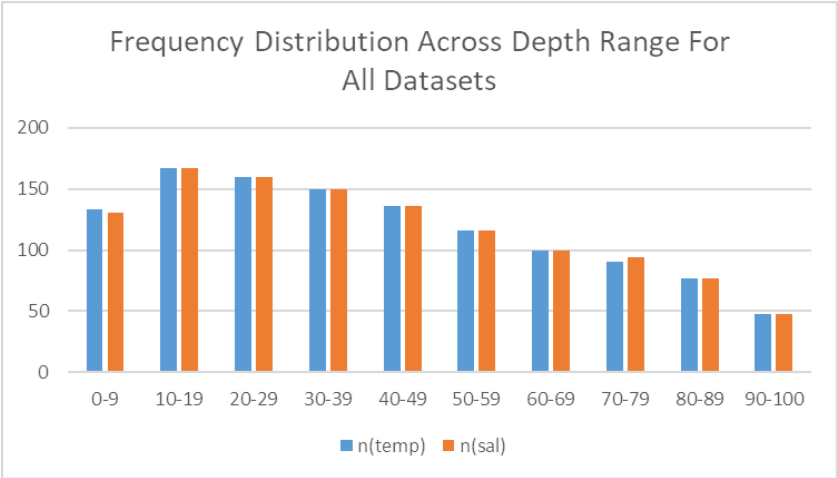

Figure 14 Frequency Distribution Across Depth Range for All Datasets

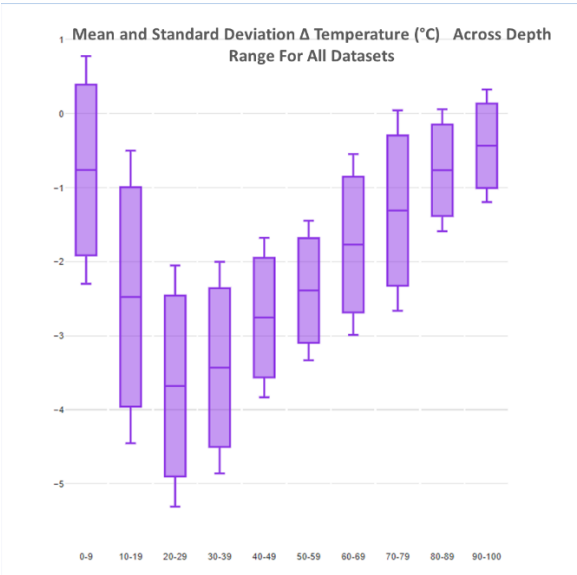

Figure 15 Mean and Standard Deviation Temperature Difference Across All Datasets

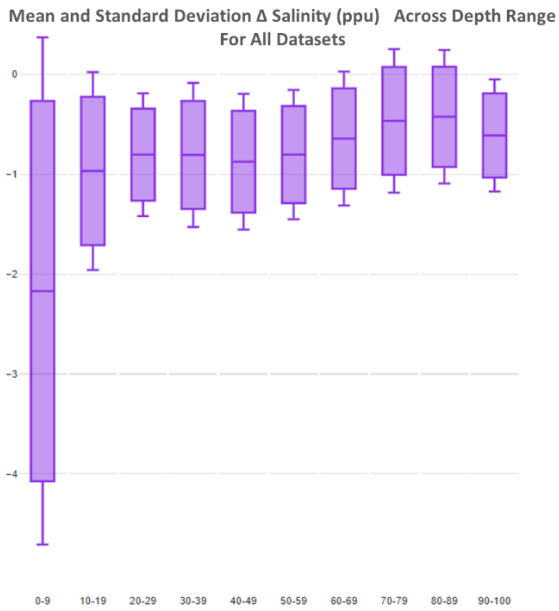

Figure 16 Mean and Standard Deviation Salinity Differences Across All Datasets

The salinity and temperature values were then used to create an SVP. The TEOS-10 sound speed algorithm is the accepted standard, however there exists several other methods to compute sound velocity (ie. Mackenzie, Del-Grosso, Chen&Millero). A quick comparison between the algorithms is given in figure 17 and 18, depicting the differences in m/s between TEOS-10 for both observed and model datasets. We can see that overall the Mackenzie calculation yields a consistent lower sound speed velocity and the Chen & Millero yields a higher sound speed velocity when compared to TEOS-10. Overall, the difference is small as the highest deviation value occurring is 0.32 m/s.

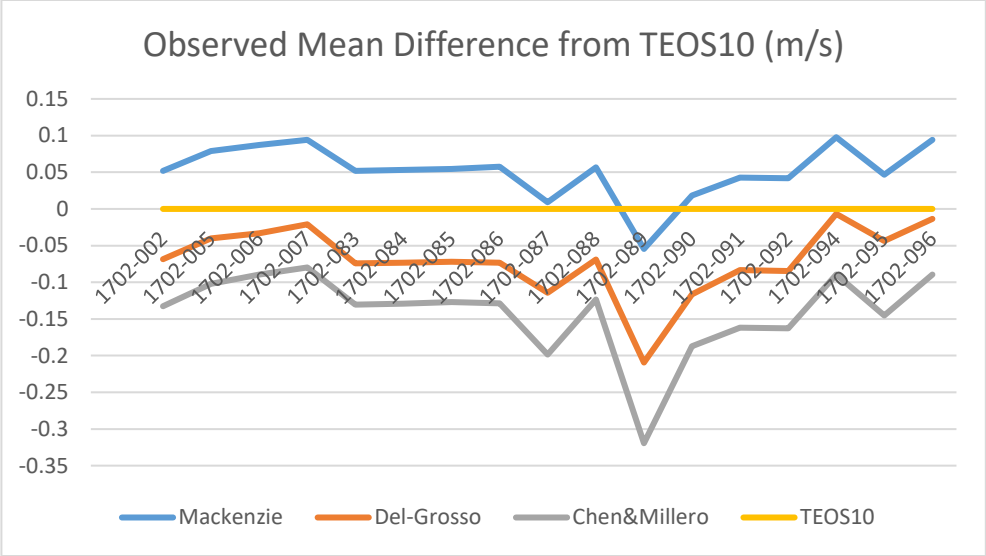

Figure 17 Observed Mean Sound Velocity Difference From TEOS-10

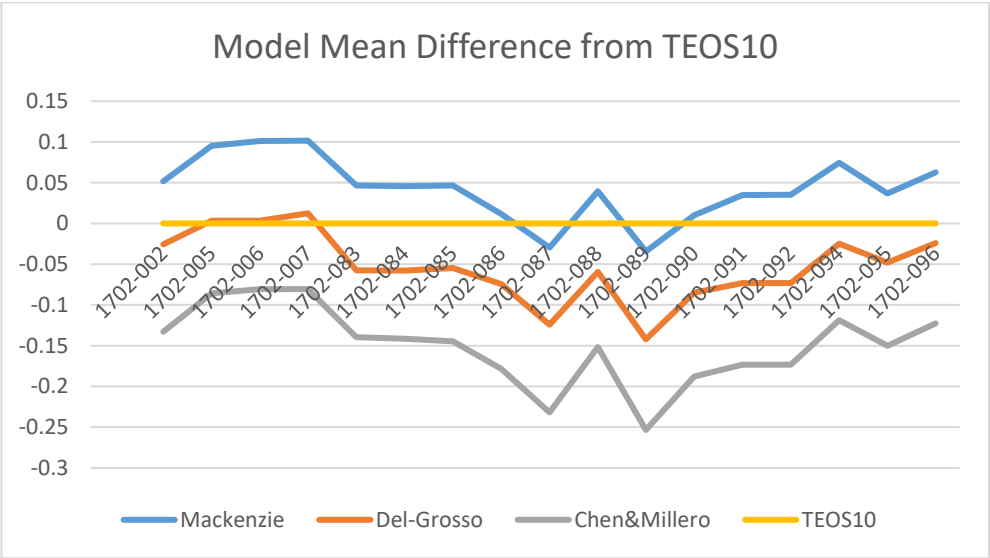

Figure 18 Model Mean Sound Velocity Difference From TEOS-10

To then finalize the comparison, raytracing was performed between the datasets to calculate the depth error that would occur between the two datasets. Since a single-beam echosounder is used in this project, raytracing was done at nadir using the TEOS-10 SVP. The travel-time was computed for the observed SVP and then using that travel time a depth was computed using the model SVP. The results of this comparison are shown in table 8. It is shown that the maximum depth difference between the datasets is 1m, the minimum depth difference is 0.03m and the average depth difference is 0.55m. This translates into a maximum, minimum and average depth error percentage of 1.55%, 0.168% and 0.76% respectively.

Table 8 Raytracing Results Comparison Between Observed and Model Depth Differences

	Depth Error (Obs vs. Model)						
Dataset	**obs_depth (m)**	**obs_owtt (s)**	**sim_depth (m)**	**depth_diff (m)**	**error%**	**lat**	**long**
1702-002	77	0.053	77.850	0.850	1.092	58.4258	-78.3035
1702-005	75	0.052	75.457	0.457	0.606	60.6961	-78.5643
1702-006	86	0.060	86.353	0.353	0.409	62.5129	-78.4889
1702-007	94	0.065	94.442	0.442	0.468	62.3669	-74.662
1702-083	100	0.070	100.758	0.758	0.753	68.3028	-101.7446
1702-084	98	0.068	98.784	0.784	0.793	68.3027	-101.7378
1702-085	93	0.065	93.798	0.798	0.851	68.2471	-101.8109
1702-086	56	0.039	56.879	0.879	1.546	68.4862	-103.4292
1702-087	42	0.029	42.453	0.453	1.067	68.3279	-102.9396
1702-088	95	0.066	95.921	0.921	0.961	68.2426	-101.795
1702-089	29	0.020	29.297	0.297	1.015	68.4906	-99.8955
1702-090	83	0.058	84.001	1.001	1.192	68.3061	-100.8015
1702-091	54	0.037	54.333	0.333	0.613	69.1707	-100.7054
1702-092	53	0.037	53.320	0.320	0.600	69.1691	-100.6952
1702-094	42	0.029	42.071	0.071	0.168	69.2716	-80.6078
1702-095	16	0.011	16.031	0.031	0.195	68.7668	-80.841
1702-096	91	0.063	91.579	0.579	0.632	65.451	-83.2584
Max				**1.001**	**1.546**		
Min				**0.031**	**0.168**		
Avg				**0.549**	**0.762**		

Overall, the observed maximum depth error of 1.546% in dataset 1702-086 does not seem significant. According to the International Hydrographic Office (IHO) Total Vertical Uncertainty (TVU) guidelines, this falls within level 1A survey standards. When calculating the error for the corresponding depth of 56m, the allowable TVU is 0.883m. The observed error is 0.879m and thus meets the requirements of a level 1A survey. The minimum depth error of 0.168% in the 1702-094 dataset, actually meets Special survey standards for TVU with an allowable error of 0.402m while we have calculated an error of 0.071m. More information on the survey standards can be found in the IHO S44 manual (International Hydrographic Organization, 2008).

The discrepancies between the observed and model depths would be a result of differing input temperature and salinity values. A larger difference in salinity and temperatures would lead to a higher calculated error % between the observed and model depths. The sound velocity algorithm should play no significant role as the algorithm was kept the same throughout the study.

Conclusion

In conclusion, we can see the use of GLONASS along with GPS to have both benefits and drawbacks when surveying in the Arctic. There was no clear winner when examining only the positional uncertainly, however GLONASS support does make a difference between throwing out data and being able to use it in some cases. Also, it can be shown from the results that using the HYCOM ocean model would be an acceptable alternative for obtaining temperature and salinity values in the absence of observed CTD casts. When converted to a SVP and used to calculate depth through the water column, the maximum depth error seen was 1.55% for shallow depth (<100m) Canadian Arctic water casts. While it is not always cost-effective or possible to obtain observed CTD casts when off-shore, these are very favorable results and show that the HYCOM model can be used and thus reduce time and costs during a survey. The GNSS and SVP processing methods established for the CSB project will allow for the automated data processing and metadata extraction, all while improving data quality. The novel use of a crowd-sourced approach along with automated processing will help further the onus of the mapping of the Canadian Arctic.

Works Cited

Church, I., Brucker, S., Hughes, J., Haigh, S., Bartlett, J., & Janzen, T. (2009). Developing Strategies to Facilitate Long Term Seabed Monitoring in the Canadian Arctic using Post Processed GPS and Tidal Models. *US Hydro*.

Collins, K., Hannah, C., & Greenberg, D. (2011). *Validation of a High Resolution Modelling System for Tides in the Canadian Arctic Archipelago.* Dartmouth.

Grosso, V. D. (1974). New equation for the speed of sound in natural waters (with comparisons to other equations). *The Journal of the Acoustical Society of America 56, 1084*.

Guo, Q. (2014). Precision comparison and analysis of four online free PPP services in static positioning and tropospheric delay estimation. *GOS Solutions*, 537-544.

Huber, K., Heuberger, F., Abert, C., Karabatic, A., Weber, R., & Berglez, P. (2010). PPP: Precise Point Positioning – Constraints and Opportunities.

Intergovernmental Oceanographic Commission. (2010). *The International Thermodynamic Equation of Seawater - 2010: calculation and use of thermodynamic properties.* UNESCO.

International Hydrographic Organization. (2008). *IHO Standards for Hydrographic Surveys 5th Ed., N44.* International Hydrographic Bureau.

International Hydrographic Organization. (2018). *Guidance on Crowdsourced Bathymetry (Draft).*

Jensen, A., & Sicard, J.-P. (2010). Challenges for Positioning and Navigation in the Arctic. *Coordinates*.

Langley, R. (1999). Online Precise Point Positioning. *GPS World*.

Langley, R. (2008). Online Precise Point Positioning. *GPS World*.

Mackenzie, K. V. (1981). Nine-term equation for sound speed in the oceans. *The Journal of the Acoustical Society of America 70, 807*.

Malinowski, M., & Kwiecien, J. (2016). A Comparative Study of Precise Point Positioning (PPP) Accuracy Using Online Services. *Sciendo*, 15-30.

Matteo, N., Morton, Y., Chandrasekaran, P., & Van Graas, F. (2009). Higher Order Ionosphere Errors at Arecibo, Millstone, and Jicamarca. International Technical Meeting of The Satellite Division of the Institute of Navigation (ION GNSS 2009) (pp. 2739-2740). Savannah: ION GNSS.

McDougall, T.J. and P.M. Barker, 2011: Getting started with TEOS-10 and the Gibbs Seawater (GSW) Oceanographic Toolbox, 28pp., SCOR/IAPSO WG127, ISBN 978-0-646-55621-5

Medwin, H. (1975). Speed of sound in water: A simple equation for realistic parameters. *The Journal of the Acoustical Society of America 58, 1318*.

Metzger, Smedstad, Thoppil, Hurlburt, Cummings, Wallcraft, . . . Franklin. (2014). US Navy Operational Global Ocean and Arctic Ice Prediction Systems. *Oceanography*, 32-43.

Mirjam Snellen, J. D. (2008). Correcting bathymetry measurements for water sound speed effects using inversion theory. *The Journal of the Acoustical Society of America*.

Monge, M., Clara de Lacy, M., & Radicella, S. (2011). On the effects of the ionospheric disturbances on precise point positioning at equatorial latitudes. *GPS Solutions*, 381-390.

Pike, & Beiboer. (1993). A Comparison Between Algorithms for the Speed of Sound in Seawater. *Hydrographic Society*.

Reid, T., Walter, T., Blanch, J., & Enge, P. (2015). GNSS Integrity in the Arctic. *The 28th International Technical Meeting of the Satellite Division of The Institute of Navigation (ION GNSS+ 2015).* Tampa.

Wells, D., Beck, N., Delikaraoglou, D., Kleusberg, A., Langley, R., & Vanicek, P. (1999). *GUIDE TO GPS POSITIONING*. New Brunswick: Department of Geodesy and Geomatics Engineering, University of New Brunswick.

Wilson, W. D. (1960). Equation for the Speed of Sound in Sea Water. *The Journal of the Acoustical Society of America 32(10)*.